Nuclear Instruments and Methods in Physics Research B 270 (2012) 12–18

Contents lists available at SciVerse ScienceDirect

Nuclear Instruments and Methods in Physics Research B

journal homepage: www.elsevier.com/locate/nimb

In situ formation of cosmogenic ^{14}C by cosmic ray nucleons in polar ice

Aleksandr Nesterenok *, Victor Naidenov

Ioffe Physical-Technical Institute, 26 Polytechnicheskaya St., 194021 Saint Petersburg, Russia
St. Petersburg State Polytechnic University, 29 Polytechnicheskaya St., 195251 Saint Petersburg, Russia

ARTICLE INFO

Article history:
Received 30 May 2011
Received in revised form 29 September 2011
Available online 8 October 2011

Keywords:
Cosmic rays
Polar ice
Radiocarbon
In situ production

ABSTRACT

We study interactions of cosmic ray particles with the Earth's atmosphere and polar ice focusing on in situ formation of radiocarbon in polar ice. We calculate the production rate of the nuclide for sea level high geomagnetic latitudes using various sets of cross section data and compare our results with experimental data. The effective attenuation length of cosmic ray spallation reactions in ice is found to be 130 g/cm^2 for high geomagnetic latitudes. Accurate determination of this parameter is important for radiocarbon concentration calculations for ice samples from ablating areas of ice sheet. The recalculation of the radiocarbon production rates for different glacier elevations is discussed.

1. Introduction

Interactions of cosmic rays with the Earth's atmosphere produce cascades of secondary particles and a variety of cosmogenic nuclides. Some of the particles created in these cascades can reach the surface of the Earth and induce nuclear reactions with the appearance of some cosmogenic nuclides. The records of radionuclides produced in the atmosphere and deposited in natural archives have been used as a proxy of changes in the primary cosmic ray flux in the past [1]. However, the cosmic ray signal in these records is in some cases obscured by natural processes on the Earth.

The radiocarbon deposition in polar ice is a complex process depending on many factors. Radiocarbon is incorporated in ice by trapping atmospheric gases during transformation of firn[1] into glacier ice. In addition, nuclear interactions of energetic neutrons and muons of cosmic rays create ^{14}C in firn and ice, as these are accumulated and in ablating ice as it outcrops. This additional in situ produced ^{14}C appears to be oxidized to ^{14}CO and $^{14}CO_2$ [2]. In situ ^{14}C has been used to determine the ablation rate of outcropping ice in Antarctica [3–5], and the presence of an in situ signal in an accumulating ice has been confirmed in experiments [6–11].

The factors which control deposition of in situ ^{14}C in polar ice are discussed in Refs. [2,9,12]. The production rate of in situ ^{14}C in ice depends on the intensity of cosmic ray flux at the polar site. The main parameter controlling the intensity of cosmic rays at polar latitudes is the level of solar activity. Changes in the geomagnetic field do not affect the cosmic ray flux at high geomagnetic latitudes. Hence, the in situ ^{14}C record in polar ice can provide a direct measure of changes in solar activity in the past [9]. An important problem related to in situ ^{14}C is the efficiency of retention in firn grains during ice formation. Some amount of ^{14}C, in situ produced in firn grains, can be lost via the gas diffusion between firn grains and firn air [2,12]. Moreover, sublimation and condensation cycles during firn grain metamorphism have the potential to release species dissolved in ice [10,12,13]. The accurate estimation of the in situ ^{14}C production rates in ice is necessary for accurate determination of deficiencies in experimental concentrations and, hence, to better understand processes affecting the efficiency of in situ ^{14}C retention in firn grains.

There is no consensus in the literature about radiocarbon production rates in ice and published values differ in two times (for example, see Refs. [6,11]). In the present work, we study interactions of cosmic rays with the Earth's atmosphere and ice exposed at the Earth's surface. The emphasis of this work is on radiocarbon in situ formation by cosmic ray nucleons in polar ice. The differences between our results and previous works are discussed.

2. Calculational model

2.1. Galactic cosmic rays

Cosmic rays at energies above several hundred MeV per nucleon are mostly of galactic origin, about 90% of particles being protons and 10% helium nuclei. The particle fraction of heavier nuclei does not exceed 1%. The flux of galactic cosmic rays is highly isotropic.

* Corresponding author at: Ioffe Physical-Technical Institute, 26 Polytechnicheskaya St., 194021 Saint Petersburg, Russia. Tel.: +7 812 292 71 80; fax: +7 812 5504890/2971017.

E-mail addresses: alex-n10@yandex.ru (A. Nesterenok), Naidenov@cycla.ioffe.ru (V. Naidenov).

[1] Firn is an intermediate stage in the transformation of snow to glacier ice.

0168-583X/$ - see front matter
doi:10.1016/j.nimb.2011.09.026

At energies below few GeV per nucleon the flux of galactic cosmic rays in space at the Earth's orbit depends on the level of solar activity. The differential energy spectrum of cosmic ray nuclei of type i in the force field approximation is given by [14]:

$$J_i(E) = J_{i,\mathrm{LIS}}(E+\Phi_i)\frac{E(E+2m_pc^2)}{(E+\Phi_i)(E+\Phi_i+2m_pc^2)}, \quad (1)$$

where $J_{i,\mathrm{LIS}}(E)$ gives the local interstellar spectrum of nuclei i, E is kinetic energy of nucleus per nucleon, m_pc^2 is proton's rest-mass energy, $\Phi_i = (eZ_i/A_i)\varphi$, Z_i and A_i are nucleus charge and mass numbers, respectively, e is the elementary charge, and φ is the modulation potential of cosmic rays in the heliosphere. We take the parameterization of the local interstellar spectrum from Ref. [15]:

$$J_{i,\ \mathrm{LIS}}(E) = C_i\frac{p(E)^{-2.78}}{1+0.487p(E)^{-2.51}}, \quad (2)$$

where E is expressed in GeV per nucleon, $p(E) = \sqrt{E(E+2m_pc^2)}$, C_i is the normalization factor; $C_p = 1.9\times10^4$ (m^2 s sr GeV)$^{-1}$ for protons, and $C_{\mathrm{He}} = 9.5\times10^2$ (m^2 s sr GeV/nucleon)$^{-1}$ for helium nuclei.

The modulation potential φ, reconstructed for the period of 1951–2004 years using the data from the worldwide neutron monitor network, ranges from 0.3 to 1.3 GV, the mean value of φ is 0.69 GV [15]. We adopt this mean value of the modulation potential in our simulations. The present-day mean solar modulation appears to be similar to the long-term mean, see discussion and references in Ref. [16]. Note, that for solar modulation parameters within 25% of the modern mean, cosmogenic neutron fluxes in the atmosphere vary about ±5% at high latitudes [17].

The Z/A ratio determines the shape of the differential energy spectrum at low energies. This ratio is close to 1/2 for nuclei with charge numbers $Z \geqslant 2$. The contribution of all $Z \geqslant 2$ nuclei to particle cascade in matter is determined by applying a scaling factor k to the results, obtained for α-particles, where k is the ratio of nucleon number densities of all $Z \geqslant 2$ nuclei to α-particles in the galactic cosmic rays. The data on energy spectrum of cosmic-ray nuclei from Ref. [18] give $k = 1.44$. All $Z = 2$ particles are treated as ^{4}He nuclei, i.e., the abundance of ^{3}He in the helium flux is neglected.

The vertical cutoff rigidities for geomagnetic latitudes $\lambda > 60°$ generally do not exceed 1 GV [19]. This cutoff value corresponds to proton kinetic energy about 430 MeV and α-particle kinetic energy about 125 MeV/nucleon. Particles at these energies provide a minor contribution to the cascade processes in the atmosphere. Hence, cosmic ray fluxes in the atmosphere are unaffected by changes in the geomagnetic field at high geomagnetic latitudes. We disregard the effect of geomagnetic cutoff on energy spectra of cosmic rays because we consider the radiocarbon production in ice at high geomagnetic latitudes.

2.2. Model of the Earth's atmosphere and surface

The Earth is modeled as a sphere of a radius of 6371 km. The Earth's surface is assumed to contain H_2O ice with the density of 0.917 g/cm^3.

The atmosphere is considered as a spherical shell of 100 km thickness. The chemical composition of the air (by mass) is nitrogen 75.5%, oxygen 23.2% and argon 1.3%. At altitudes from the surface to about 80 km the chemical composition is nearly constant due to atmospheric mixing [20]. The total thickness of the atmosphere is taken to be equal to the atmospheric depth of 1034 g/cm^2 at sea level. The atmosphere is divided into concentric subshells with a thickness of 15 g/cm^2 and constant air density within one subshell. Additional division is done near air–ice interface. The dependence of air density on altitude is taken from the COSPAR reference atmosphere data for high geographic latitudes $\lambda > 60°$N [21].

The cosmic ray particle flux at a given altitude is controlled by the mass of atmosphere (atmospheric depth) traversed by the particles. To apply simulation results to a given location on the Earth one needs to convert site altitude to atmospheric depth using pressure data or appropriate air density dependence on altitude [22–24].

2.3. Physics input

Particle fluxes in matter are calculated using simulation toolkit GEANT4 9.4 [25]. The processes included are those of production, propagation and interaction of baryons (nucleons, short-lived baryons and their antiparticles), mesons (pions and kaons), light nuclei, leptons (electrons, positrons, muons) and gamma rays. Standard electromagnetic processes, photonuclear and electronuclear processes are taken into account [26]. Particles of electron-photon component with energies less than 10 MeV are excluded from calculations. Low-energy and high-energy parameterized models are used to describe inelastic scattering of hadrons and nuclei. The Bertini intranuclear cascade model is employed for describing nucleon–nucleus and meson–nucleus inelastic scattering at hadron energies up to 6 GeV. The binary intranuclear cascade model is adopted for inelastic scattering of light nuclei. Processes of negative meson capture, neutron capture and neutron fission are included. High precision neutron models are used for simulating neutron–nucleus interactions. These models are based on the G4NDL data library (version 3.14) that comes largely from the ENDF-B VI and JENDL libraries for neutron energies below 20 MeV. For neutron energies in the range from 20 MeV to about 3 GeV the JENDL/HE cross section data are employed.

2.4. Calculation of particle fluxes

Let us define the angle-integrated differential flux of particles of type i:

$$I_i^{\mathrm{diff}}(E) = \int_{4\pi} d\Omega J_i\,(E),$$

where J_i (E) is a directed differential flux or differential energy spectrum of particles i. Let us introduce also the angle- and energy-integrated flux of particles i with energies above E:

$$I_i^{\mathrm{int}}(E) = \int_E^\infty dE'\, I_i^{\mathrm{diff}}(E') = \int_E^\infty dE' \int_{4\pi} d\Omega J_i\,(E').$$

The 4π angle-integrated integral flux of galactic cosmic rays is found to be 2.66 cm^{-2} s^{-1} for protons, and 0.27 cm^{-2} s^{-1} for helium nuclei at $\varphi = 0.69$ GV and $E = 100$ MeV/nucleon employing the particle differential energy spectra (1) and (2).

The flux of galactic cosmic rays passing through unit area of the upper atmosphere boundary is:

$$F_{0i} = \int_{2\pi} \mathrm{d}\Omega \cos\theta \int_E^\infty \mathrm{d}E' J_{0i}\,(E') = \pi \int_E^\infty \mathrm{d}E' J_{0i}\,(E'),$$

where $J_{0i}(E)$ is directed differential flux of galactic cosmic ray nuclei of type i at the Earth orbit, θ is the angle between particle momentum and nadir point. The distribution over θ of the primary cosmic rays penetrating the atmosphere satisfies the relation $\mathrm{d}F_{0i}/\mathrm{d}\cos\theta \sim \cos\theta$.

Angle-integrated differential flux of particles i with energy E in matter at a depth z is calculated according to:

$$I_i^{\mathrm{diff}}(E,z) = \frac{F_{0p}}{N_{0p}\Delta E}\sum_l \frac{1}{|\cos\theta_{li}|} + k\frac{F_{0\alpha}}{N_{0\alpha}\Delta E}\sum_l \frac{1}{|\cos\theta_{li}|},$$

where N_0 is the number of primary particles (protons or α-particles) for which the cascade simulations are performed, the inner summation is done over all particles i crossing a fixed level in matter at depth z and having energies in the range $(E - \Delta E/2, E + \Delta E/2)$, θ_{li} being the particle zenith angle, $k = 1.44$. Particles with $|\cos\theta_{li}| < 0.001$ for atmosphere levels and those with $|\cos\theta_{li}| < 0.01$ for ice levels are excluded from the sum.

We have simulated five million particle cascades initiated by protons and two million cascades initiated by α-particles of galactic cosmic rays. Particle energy has been chosen at random according to the particle differential energy spectra (1) and (2). We have considered primary particles with energies between 100 MeV/nucleon and 1000 GeV/nucleon. Primary α-particles with energies above 10 GeV/nucleon have been treated as four unbound nucleons.

Simulations have been performed at the Saint-Petersburg branch of Joint Supercomputer Center of the Russian Academy of Sciences.

2.5. Cross sections for ^{14}C in situ formation in ice

The production rate of the cosmogenic nuclide in matter at a depth z is

$$P(z) = \sum_k N_k \sum_i \int_0^\infty dE\, \sigma_{ik}(E) I_i^{\mathrm{diff}}(E, z),$$

where N_k is the number density of atoms of the target element k, $\sigma_{ik}(E)$ is the cross section for the nuclide production from the target element k by particles i with energy E, and $I_i^{\mathrm{diff}}(E, z)$ is the angle-integrated differential flux of particles i with energy E at location z.

The formation of ^{14}C in polar ice by cosmic ray nucleons is mainly due to spallation of oxygen nuclei induced by energetic neutrons:

$$^{16}\mathrm{O} + \mathrm{n} \to {}^{14}\mathrm{C} + \mathrm{X},$$

where X denotes all possible reaction products. Fig. 1 shows the experimental and theoretical excitation functions for this reaction. Experimental cross sections for neutron energies up to 33 MeV are taken from Ref. [27] – circles in Fig. 1. There are no reliable experimental cross sections for higher neutron energies due to complexity of such experiments; although some measurements were made [28]. Cross sections for high-energy neutrons were kindly provided by Dr. Robert C. Reedy from the University of New Mexico in USA – triangles in Fig. 1. These data are based on the cross sections of corresponding proton induced reaction. Kim et al. [29] used Reedy's cross sections to model ^{14}C formation in the meteorite Knyahinya and in the Apollo 15 deep drill core. Measurements and calculations agree within 15–25%. The excitation function for the reaction in question was also provided by Dr. Rolf Michel from the University of Hannover in Germany – the solid line in Fig. 1.

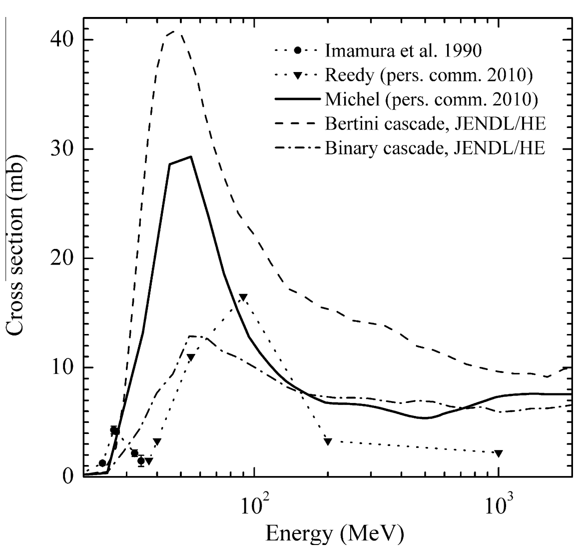

Fig. 1. Excitation functions for the reaction $^{16}O(n, X)^{14}C$. Circles are for experimental cross sections from Ref. [27], triangles – cross sections, provided by R.C. Reedy, solid line – the excitation function, provided by R. Michel. Dashed line is for the excitation function, which has been derived from Bertini intranuclear cascade simulations, dash-dot line – the excitation function, which has been derived from binary intranuclear cascade simulations.

The results of GEANT4 simulations of ^{14}C formation from spallation of oxygen by neutrons are shown in Fig. 1. We have used the total inelastic cross sections provided by JENDL/HE. Two models of neutron inelastic scattering have been used, the Bertini intranuclear cascade model and the binary intranuclear cascade model. The models differ in description of particle–particle interactions. In particular, the binary intranuclear cascade model takes into account formation of resonant particles in nucleon–nucleon and meson–nucleon collisions [26]. Statistical errors of the simulation results do not exceed 0.3 mb. The energy distribution of product nuclei has been also determined (see Section 3.5).

The ^{14}C production rate in ice due to proton induced spallation of oxygen, $^{16}O(p, 3p)^{14}C$, is calculated. The reaction cross sections are taken from Refs. [30,31]. The contribution of the reactions $^{17}O(n, \alpha)^{14}C$ and $^{18}O(n, \alpha n)^{14}C$ to radiocarbon formation is estimated to be small.

3. Results and discussion

3.1. Neutron energy spectrum at the atmosphere–ice interface

Fig. 2 shows calculated neutron angle-integrated differential flux at the atmosphere–ice interface at sea level. For comparison, we present the angle-intergrated differential fluxes of neutrons from Refs. [32,33]. The data from Ref. [32] are the results of neutron spectrum measurements scaled to sea level high geomagnetic latitudes and mid-level solar modulation. Gordon et al. [32] estimate the uncertainty in the response functions for the detectors to be 10–15% above 150 MeV and lower for lower energies, producing a similar uncertainty of the measured data. The data from Ref. [33] are the results of Monte Carlo simulations using the PHITS code and the nuclear data library JENDL/HE. The spectrum was

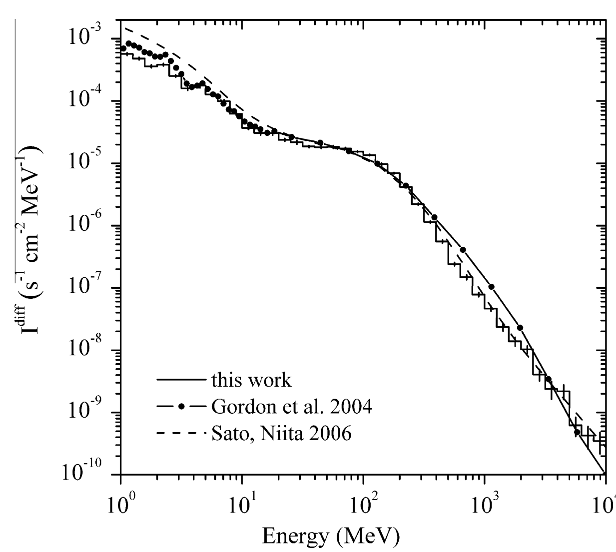

Fig. 2. The angle-integrated differential neutron flux at sea level. Step-like curve shows calculated results, error bars show statistical uncertainty. Circles connected by line present measured spectrum [32]. Dashed line is for calculated spectrum from Ref. [33].

calculated for semi-infinite atmosphere without considering air–ground interface.

The differences between calculated and measured neutron spectra at low energy region can be explained by air–ground interface effects. The neutron spectrum at the ground level depends on the landscape geometry and the chemical composition of the ground [33,34]. There is significant dependence of the neutron spectrum at low energies on the weight fraction of hydrogen or water in the ground, the neutron fluxes being lower for higher hydrogen content [33]. The disturbance of the neutron spectrum at the ground level by local geometry effects (chemical composition) decreases with energy, being no more than 30% at neutron energies 10 MeV [33].

The measured and calculated fluxes agree within 30% for neutron energies from 10 to 300 MeV. The neutron spectrum has a plateau in this energy region. Neutrons at these energies provide the main contribution to the formation of cosmogenic nuclides in spallation reactions. The differences between calculated and measured fluxes at higher energies become substantial and reach 200%. The discrepancy may be caused by the fact that the total inelastic cross sections JENDL/HE used in simulations are overstated in this energy region. The 15% difference in the total interaction cross sections can lead to twofold difference in the particle fluxes at 5–6 absorption mean free paths. The fact that the spectrum from Ref. [33] has similar behavior at energies in question strengthens this conclusion.

The contribution of particle cascades initiated by nuclei $Z \geqslant 2$ of galactic cosmic rays to the particle fluxes in the atmosphere has been found to be 25% at sea level for high geomagnetic latitudes.

3.2. Cosmogenic ^{14}C in situ formation rate at the ice surface

The calculated cosmogenic ^{14}C production rates in ice exposed at the Earth's surface are given in the Table 1. The results are presented for the calculated neutron and proton differential fluxes and different cross sections. Statistical errors of these calculations are expected to be 1–3%. The differences in the calculated and measured neutron fluxes result in about 10% difference in ^{14}C production rates in ice. For comparison, the production rates of ^{14}C in ice from references [5,35–37] are presented in the Table 1.

Measurements of number densities of cosmogenic nuclides in samples from stable, continuously exposed geological surfaces enable to derive production rates of cosmogenic nuclides in rocks. The estimates of ^{14}C in situ production rates in quartz for sea level high latitudes range in 15–18 atoms/g/yr [16,38]. The result depends on the production rate scaling model used to recalculate the measured rate at a given location to sea level high latitudes. At sea level high latitudes stopped negative muons and fast muons account for about 15% of ^{14}C production in quartz [37]. The production of ^{14}C in SiO_2 by nucleons was found to be predominantly (about 95%) from oxygen [39]. Measured ^{14}C production rates in quartz correspond to the nuclide production rate by cosmic ray nucleons in ice of about 21–25 atoms/g/yr for sea level high latitudes. The surface production rates of ^{14}C in ice given in Refs. [5,37] are based on the measurements of radiocarbon production rate in quartz from Ref. [40]. The production rates of ^{14}C in quartz reported in Ref. [40] are about 15–20% higher than the values published more recently in Ref. [38]. Further refinement of ^{14}C production rates in quartz is necessary for more accurate constraints to be imposed on nuclide production rate in ice. Cross sections provided by R.C. Reedy and the excitation function calculated using the binary intranuclear cascade model lead to the radiocarbon production rates in ice which are in good agreement with measured production rates in quartz.

According to our simulations, the spallation of oxygen by protons contributes about 2–3% in the total production rate of ^{14}C by cosmic ray nucleons in ice for sea level high geomagnetic latitudes. The radiocarbon production rate in ice calculated using the proton angle-integrated differential spectrum from Ref. [41] is found to be lower – about 0.25 atoms/g/yr.

3.3. Depth dependence of ^{14}C production rate in ice

The nucleon fluxes in ice decrease roughly exponentially with increasing depth. At high energies the spectral shapes of differential nucleon fluxes change little with increasing depth. The dependence of radiocarbon production rate on depth is expected to be similar to the depth dependence of the high energy neutron flux in ice. The production rate of a cosmogenic nuclide at a depth z below the ice surface can be expressed as:

$$P(z) = P_0 \exp(-z/\Lambda_{\text{ice}}),$$

where P_0 is the production rate at the ice surface, Λ_{ice} is the thickness of a slab of ice required to attenuate the energetic cosmic ray nucleon flux by a factor of $e \approx 2.72$.

Fig. 3 shows the calculated production rate of ^{14}C as a function of ice depth. The excitation function of the oxygen spallation evaluated using the binary intranuclear cascade model has been used in nuclide formation rate calculations. The parameters of exponential fit – the solid line in Fig. 3 – are the following: P_0 = 26.3 atoms/g/yr and Λ_{ice} = 128 g/cm^2. For comparison, the depth dependences of the radiocarbon production rate in ice according to Refs. [35–37] are presented in Fig. 3.

The depth dependence of neutron flux in terrestrial rocks was found in Refs. [34,42] to show a relatively flat profile near the surface–air interface to a depth of about 12 g/cm^2. According to our simulations such interface effect does exist for protons but not for high energy neutron flux. The reason for such discrepancy may lie in different chemical composition of the ground in our

Table 1
Cosmogenic ^{14}C in situ production rates at the ice surface for sea level high latitudes.

The results obtained in this work		
Spallation reaction	Cross section data	Prod. rate (atoms/g/yr)
^{16}O(n, X)^{14}C	[27], R.C. Reedy (pers. comm. 2010)	26
	R. Michel (pers. comm. 2010)	39
	Bertini cascade, JENDL/HE	66
	Binary cascade, JENDL/HE	26
^{16}O(p, 3p)^{14}C	[30,31]	0.6
The results published earlier		
References		Total prod. rate (atoms/g/yr)
[35,36]		15
[37]		31
[5]		27 ± 7

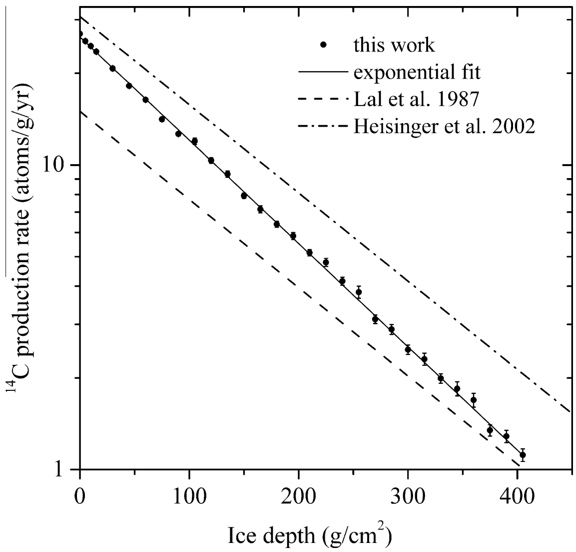

Fig. 3. The production rate of ^{14}C by cosmic ray nucleons in ice as a function of depth for sea level high geomagnetic latitudes. Circles show calculated results, error bars show statistical uncertainty. Solid line presents approximation by exponential function. Dashed line is for the depth dependence of ^{14}C production rate as stated in Ref. [35], dash-dot line – the depth dependence of ^{14}C production rate according to Ref. [37].

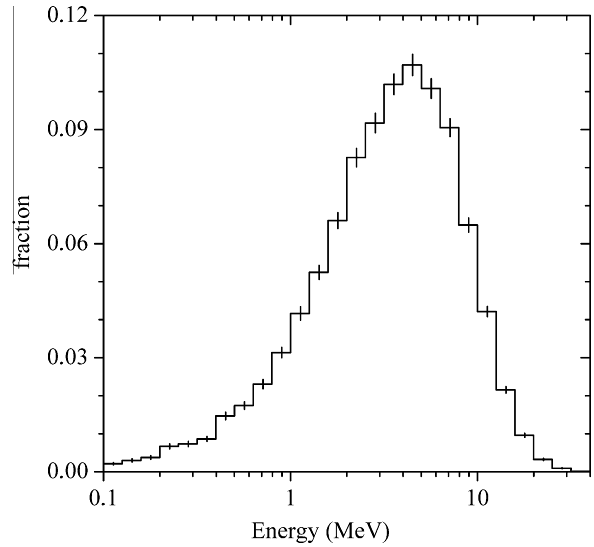

Fig. 4. Energy distribution of ^{14}C nuclei formed in neutron induced spallation of oxygen. The y-axis shows the fraction of ^{14}C nuclei per energy bin. Error bars present statistical uncertainty.

model and that of Refs. [34,42] and in different cross section libraries used.

The effective attenuation length of high energy nucleons in ice Λ_{ice} has been found to be 130 g/cm^2 which is equal to the value of the parameter in the lower troposphere at high geomagnetic latitudes (see Section 3.4 and references therein). The effective attenuation length of high energy spallation reactions was taken to be 150–160 g/cm^2 in previous studies of ^{14}C in polar ice [3–12,35,36]. The value of the effective attenuation length of high energy nucleons in ice was taken in Ref. [35] to be equal to the value of the parameter in the troposphere at high latitudes but an overstated value of the parameter was used.

The concentration of ^{14}C produced by cosmic ray nucleons in ablating ice is proportional to the production rate at depth in question [3–5]. The 15% error in Λ_{ice} leads to 50% error in calculated concentrations of ^{14}C at depth of $3\Lambda_{ice}$ in ice. Choosing the correct value for this parameter is crucial for radiocarbon studies of ablating areas of ice sheet.

3.4. Altitude dependence of ^{14}C production rate in ice

Production rates of cosmogenic nuclides at the Earth's surface are controlled by the intensity of cosmic ray particles, which changes with elevation and geomagnetic coordinates. Differences in cosmic ray intensity at a sample site and a reference site with known production rate are accounted for by multiplying the reference production rate by a scaling factor. For the nuclide production rate in ice exposed at the Earth's surface at altitude h for high geomagnetic latitudes one can define:

$$P_h = P_0 \exp\left(\frac{1034 - x(h)}{\Lambda_{atm}}\right),$$

where P_0 is the sea level rate, $x(h)$ is the atmospheric depth in g/cm^2 at altitude h, Λ_{atm} is the effective attenuation length of high energy nucleon flux in the atmosphere. There are a number of production rate scaling models which are based on different cosmic ray flux measurements and differ in description of geomagnetic field and atmospheric pressure [16,24,43–46]. The model of Ref. [43] gives values of the parameter Λ_{atm} ranging from 110 to 140 g/cm^2 for high geomagnetic latitudes and altitudes below 6 km. More recent models from Refs. [24,44–46] provide a value of about 130 g/cm^2 for the parameter Λ_{atm} for high geomagnetic latitudes. The 1σ uncertainty of +5/-2% is recommended in Ref. [45] for the parameter Λ_{atm}. Our simulations of particle cascades in the atmosphere provide a slightly higher value of 135 g/cm^2 for the effective attenuation length of high energy neutron flux for altitudes below 4 km which is within the measurement errors of the parameter.

3.5. Energy distribution of daughter nuclei ^{14}C

Fig. 4 shows energy distribution of product nuclei ^{14}C formed in neutron-induced spallation of oxygen. The binary intranuclear cascade model has been used in simulations. The results are for the angle-integrated differential neutron flux at sea level. Carbon nuclei formed in the spallation have initial energies up to several MeV and higher. Nuclei lose energy by ionization and collisions with water molecules. Before stopping, the ^{14}C atom or ion may induce chemical reactions; simple carbon compounds may be formed such as CO, CO_2, CH_4, CH_2O and other molecules [47]. The studies of in situ ^{14}C in polar ice have been focused mainly on carbon monoxide and dioxide as the main hot carbon chemistry products. Measurements of the partitioning of these two species have given ^{14}CO:$^{14}CO_2$ ratios from 0.1 to 1.5 [2,9]. Accurate determination of radiochemical yields of ^{14}C hot reaction products is necessary for radiocarbon dating of polar ice samples [11] and for studies of $^{14}CH_4$ trapped in polar ice [48]. Calculated energy distribution of daughter nuclei ^{14}C can be used as an input parameter for simulations of chemistry of hot atoms.

4. Conclusions

The cosmic ray cascades in the atmosphere and their interactions with ice on the Earth's surface have been simulated. The neutron and proton differential fluxes in the atmosphere and ice are calculated. Cosmic-ray neutrons with energies in the range 30–300 MeV provide the main contribution to the formation of radiocarbon in oxygen spallation reactions (about 80–90%). Calculated and measured neutron differential fluxes in the atmosphere agree within 30% for the energy region of interest. The agreement between simulation results and the experimental data for atmospheric fluxes can be considered as an indirect proof of the validity of the simulations for ice.

The ^{14}C in situ production rate in ice for sea level high geomagnetic latitudes is found using calculated differential nucleon fluxes. The result strongly depends on the excitation function employed for oxygen spallation by neutrons. Cross sections provided by R.C. Reedy and the excitation function calculated using the binary intranuclear cascade model lead to the radiocarbon production rates in ice which are in good agreement with measured production rates in quartz. The spallation of oxygen by protons is found to contribute about 1–2% in the total production rate of ^{14}C by cosmic ray nucleons in ice for sea level high geomagnetic latitudes. The effective attenuation length of high energy spallation reactions in ice is found to be 130 g/cm^2 for high geomagnetic latitudes, which is lower than the values accepted in previous studies of in situ ^{14}C in polar ice. The result is important for radiocarbon concentration calculations for ice samples from ablating areas of ice sheet.

Acknowledgments

We are grateful to Robert C. Reedy and Rolf Michel for sharing with us the cross section data. We thank Janet Sisterson from Francis H. Burr Proton Therapy Center in Boston for her advice and detailed description of the cross section measurements she made. We thank our colleague Vladimir Levchenko for valuable comments and suggestions. We would like to acknowledge the language help of our colleagues D.G. Yakovlev and A.Yu. Potekhin. This work was supported by Ministry of Education and Science of Russian Federation (contract # 11.G34.31.0001 with SPbSPU and leading scientist G.G. Pavlov).

We thank anonymous reviewer for valuable comments and suggestions.

References

[1] K.G. McCracken, J. Beer, F.B. McDonald, The long-term variability of the cosmic radiation intensity at Earth as recorded by the cosmogenic nuclides, ISSI Scientific Reports Series 3 (2005) 83–97.
[2] A.M. Smith, V.A. Levchenko, D.M. Etheridge, D.C. Lowe, Q. Hua, C.M. Trudinger, U. Zoppi, A. Elcheikh, In search of in situ radiocarbon in Low Dome ice and firn, Nuclear Instruments and Methods in Physics Research B 172 (2000) 610–622.
[3] D. Lal, A.J.T. Jull, D.J. Donahue, D. Burtner, K. Nishiizumi, Polar ice ablation rates measured using in situ cosmogenic ^{14}C, Nature 346 (1990) 350–352.
[4] J.J. van Roijen, R. Bintanja, K. van der Borg, M.R. van den Broeke, A.F.M. de Jong, J. Oerlemans, Dry extraction of $^{14}CO_2$ and ^{14}CO from Antarctic ice, Nuclear Instruments and Methods in Physics Research B 92 (1994) 331–334.
[5] W.J.M. van der Kemp, C. Alderliesten, K. van der Borg, A.F.M. de Jong, R.A.N. Lamers, J. Oerlemans, M. Thomassen, R.S.W. van de Wal, *In situ* produced ^{14}C by cosmic ray muons in ablating Antarctic ice, Tellus B 54 (2002) 186–192.
[6] A.J.T. Jull, D. Lal, D.J. Donahue, P. Mayewski, C. Lorius, D. Raynaud, J.R. Petit, Measurements of cosmic-ray-produced ^{14}C in firn and ice from Antarctica, Nuclear Instruments and Methods in Physics Research B 92 (1994) 326–330.
[7] D. Lal, A.J.T. Jull, G.S. Burr, D.J. Donahue, Measurements of in situ ^{14}C concentrations in Greenland ice sheet project 2 ice covering a 17 kyr time span: implications to ice flow dynamics, Journal of Geophysical Research C 102 (1997) 26505–26510.
[8] D. Lal, A.J.T. Jull, G.S. Burr, D.J. Donahue, On the characteristics of cosmogenic in situ ^{14}C in some GISP2 Holocene and late glacial ice samples, Nuclear Instruments and Methods in Physics Research B 172 (2000) 623–631.
[9] D. Lal, A.J.T. Jull, D. Pollard, L. Vacher, Evidence for large century time-scale changes in solar activity in the past 32 Kyr, based on in situ cosmogenic ^{14}C in ice at Summit, Greenland, Earth and Planetary Science Letters 234 (2005) 335–349.
[10] D. Lal, A.J.T. Jull, D.J. Donahue, G.S. Burr, B. Deck, J. Jouzel, E. Steig, The record of cosmogenic in situ produced ^{14}C in Vostok and Taylor Dome ice samples: implications for strong role of wind ventilation processes, Journal of Geophysical Research D 106 (2001) 31933–31941.
[11] A.F.M. de Jong, C. Alderliesten, K. van der Borg, C. van der Veen, R.S.W. van de Wal, Radiocarbon analysis of the EPICA Dome C ice core: no in situ ^{14}C from the firn observed, Nuclear Instruments and Methods in Physics Research B 223–224 (2004) 516–520.
[12] A.V. Nesterenok, V.O. Naidenov, Radiocarbon in polar ice: retention mechanism in firn grains, Geomagnetism and Aeronomy 51 (2011) 421–428.
[13] A.M. Grannas et al., An overview of snow photochemistry: evidence, mechanisms and impacts, Atmospheric Chemistry and Physics 7 (2007) 4329–4373.
[14] L.J. Gleeson, W.I. Axford, Solar modulation of galactic cosmic rays, Astrophysical Journal 154 (1968) 1011–1026.
[15] I.G. Usoskin, K. Alanko-Huotari, G.A. Kovaltsov, K. Mursula, Heliospheric modulation of cosmic rays: monthly reconstruction for 1951–2004, Journal of Geophysical Research 110 (2005) A12108.
[16] T.J. Dunai, Cosmogenic Nuclides: Principles, Concepts and Applications in the Earth Surface Sciences, Cambridge University Press, New York, 2010.
[17] M.E. Wiedenbeck et al., The level of solar modulation of galactic cosmic rays from 1997 to 2005 as derived from ACE measurements of elemental energy spectra, International Cosmic Ray Conference 2 (2005) 277.
[18] B. Wiebel-Sooth, P.L. Biermann, H. Meyer, Cosmic rays, VII. Individual element spectra: prediction and data, Astronomy and Astrophysics 330 (1998) 389–398.
[19] M.A. Shea, D.F. Smart, A world grid of calculated cosmic ray vertical cutoff rigidities for 1980, International Cosmic Ray Conference 3 (1983) 415.
[20] COESA – Committee on Extension to the Standard Atmosphere, US Standard Atmosphere, US Government Printing Office, Washington DC, 1976.
[21] Committee on Space Research (COSPAR). The COSPAR International Reference Atmosphere (CIRA-86), [Internet]. NCAS British Atmospheric Data Centre, 29.05.2011. Available from <http://badc.nerc.ac.uk/view/badc.nerc.ac.uk__ATOM__dataent_CIRA>.
[22] J.O. Stone, Air pressure and cosmogenic isotope production, Journal of Geophysical Research 105 (2000) 23753–23759.
[23] D. Desilets, M. Zreda, On scaling cosmogenic nuclide production rates for altitude and latitude using cosmic-ray measurements, Earth and Planetary Science Letters 193 (2001) 213–225.
[24] N.A. Lifton, J.W. Bieber, J.M. Clem, M.L. Duldig, P. Evenson, J.E. Humble, R. Pyle, Addressing solar modulation and long-term uncertainties in scaling secondary cosmic rays for in situ cosmogenic nuclide applications, Earth and Planetary Science Letters 239 (2005) 140–161.
[25] S. Agostinelli et al. (Geant4 collaboration), Geant4 – a simulation toolkit, Nuclear Instruments and Methods in Physics Research A 506 (2003) 250–303.
[26] Geant4 collaboration. Geant4 Physics reference manual, [Internet]. 29.05.2011. Available from <http://geant4.cern.ch/support/index.shtml>.
[27] M. Imamura, H. Nagai, M. Takabatake, S. Shibata, K. Kobayashi, K. Yoshiba, H. Ohashi, Y. Uwamino, T. Naakamura, Measurements of production cross sections of ^{14}C and ^{26}Al with high-energy neutrons up to E_n = 38 MeV by accelerator mass spectrometry, Nuclear Instruments and Methods in Physics Research B 52 (1990) 595–600.
[28] J.M. Sisterson et al., New neutron and proton production cross section measurements for cosmic ray studies, Lunar and Planetary Institute Science Conference Abstracts 30 (1999) 1202.
[29] K.J. Kim, J. Masarik, R.C. Reedy, Numerical simulations of production rates for ^{10}Be, ^{26}Al and ^{14}C in extraterrestrial matter using the MCNPX code, Nuclear Instruments and Methods in Physics Research B 268 (2010) 1291–1294.
[30] A.J.T. Jull, S. Cloudt, D.J. Donahue, J.M. Sisterson, R.C. Reedy, J. Masarik, ^{14}C depth profiles in Apollo 15 and 17 cores and lunar rock 68815, Geochimica et Cosmochimica Acta 62 (1998) 3025–3036.
[31] R.C. Reedy, Proton cross sections for producing cosmogenic radionuclides, Lunar and Planetary Institute Science Conference Abstracts 38 (2007) 1192.
[32] M.S. Gordon, P. Goldhagen, K.P. Rodbell, T.H. Zabel, H.H.K. Tang, J.M. Clem, P. Bailey, Measurement of the flux and energy spectrum of cosmic-ray induced neutrons on the ground, IEEE Transactions on Nuclear Science 51 (2004) 3427–3434.
[33] T. Sato, K. Niita, Analytical functions to predict cosmic-ray neutron spectra in the atmosphere, Radiation Research 166 (2006) 544–555.
[34] J. Masarik, K.J. Kim, R.C. Reedy, Numerical simulations of in situ production of terrestrial cosmogenic nuclides, Nuclear Instruments and Methods in Physics Research B 259 (2007) 642–645.
[35] D. Lal, K. Nishiizumi, J.R. Arnold, In situ cosmogenic ^{3}H, ^{14}C, and ^{10}Be for determining the net accumulation and ablation rates of ice sheets, Journal of Geophysical Research 92 (1987) 4947–4952.
[36] D. Lal, A.J.T. Jull, On determining ice accumulation rates in the past 40000 years using in situ cosmogenic ^{14}C, Geophysical Research Letters 17 (1990) 1303–1306.
[37] B. Heisinger, D. Lal, A.J.T. Jull, P. Kubik, S. Ivy-Ochs, K. Knie, E. Nolte, Production of selected cosmogenic radionuclides by muons. 2. Capture of negative muons, Earth and Planetary Science Letters 200 (2002) 357–369.
[38] B. Dugan, N. Lifton, A.J.T. Jull, New production rate estimates for in situ cosmogenic ^{14}C, Geochimica et Cosmochimica Acta 72 (2008) 231.
[39] A.J.T. Jull, P.A.J. Englert, D.J. Donahue, R.C. Reedy, D. Lal, Cosmogenic nuclide production rates: carbon-14 from neutron spallation, Lunar and Planetary Institute Science Conference Abstracts 20 (1989) 490–491.
[40] A.J.T. Jull, N. Lifton, W.M. Phillips, J. Quade, Studies of the production rate of cosmic-ray produced ^{14}C in rock surfaces, Nuclear Instruments and Methods in Physics Research B 92 (1994) 308–310.
[41] D. Kollar, Neutron cross sections and interactions of cosmic ray particles with terrestrial and extraterrestrial matter, PhD Thesis, Comenius University in Bratislava, Bratislava, 2003.
[42] J. Masarik, R.C. Reedy, Terrestrial cosmogenic-nuclide production systematics calculated from numerical simulations, Earth and Planetary Science Letters 136 (1995) 381–395.

[43] D. Lal, Cosmic ray labeling of erosion surfaces: in situ nuclide production rates and erosion models, Earth and Planetary Science Letters 104 (1991) 424–439.
[44] T.J. Dunai, Scaling factors for production rates of in situ produced cosmogenic nuclides: a critical reevaluation, Earth and Planetary Science Letters 176 (2000) 157–169.
[45] D. Desilets, M. Zreda, Spatial and temporal distribution of secondary cosmic-ray nucleon intensities and applications to in situ cosmogenic dating, Earth and Planetary Science Letters 206 (2003) 21–42.
[46] D. Desilets, M. Zreda, T. Prabu, Extended scaling factors for in situ cosmogenic nuclides: new measurements at low latitude, Earth and Planetary Science Letters 246 (2006) 265–276.
[47] K. Roessler, Suprathermal chemistry in space, in: E. Bussoletti, G. Strazzulla, P. Papali (Eds.), Solid-State Astrophysics, North Holland Press, Amsterdam, 1991, pp. 197–266.
[48] V.V. Petrenko et al., $^{14}CH_4$ measurements in Greenland ice: investigating last glacial termination CH_4 sources, Nature 324 (2009) 506–508.